RESEARCH ARTICLE

Removal of Pb²⁺ Ions from Aqueous Medium by Using Chitosan-Diatomite Composite: Equilibrium, Kinetic, and Thermodynamic Studies

Zeynep Mine ŞENOL[1]* ✉ ⓘ**, Selçuk ŞİMŞEK[2]** ✉ ⓘ

[1]Cumhuriyet University, Zara Vocational School, Department of Food Technology, 58140 Sivas, Turkey.
[2]Cumhuriyet University, Faculty of Science, Department of Chemistry, 58140 Sivas, Turkey.

Abstract: In this study, a novel, low-cost, natural, and highly effective adsorbent, chitosan (Ch) - diatomite (D) composite was synthesized. Ch-D composite was tested as an effective and alternative adsorbent for the removal of Pb²⁺ ions. The Ch-D composite was characterized by FT-IR, SEM-EDX and PZC analyses. The adsorption process of Pb²⁺ ions onto Ch-D as initial lead concentration, solution pH, temperature, contact time and recovery was investigated. From the adsorption process results, it has been observed that the highest removal efficiency is approximately 95% at a contact time of 4-hour, initial Pb²⁺ concentration of 500 mg L⁻¹ and agitation speed of 150 rpm at natural pH 4.0. The maximum Pb²⁺ adsorption capacity from the Langmuir model was found as 0.154 mol kg⁻¹ at 25 °C. Besides, adsorption kinetics was also explained with pseudo-first-order models. Adsorption thermodynamics have shown that Pb²⁺ adsorption onto Ch-D is possible, spontaneous and exothermic. Ch-D composite can become an alternative adsorbent for the treatment of lead ions in the wastewater.

INTRODUCTION

Industrial wastewater causes heavy metal pollutions in the environment. Nowadays, the removal of heavy metals and pollutions from wastewater is very important (1). Heavy metals and pollutants cause health problems in living organisms. Among these heavy metals, lead is an inhibitor of metabolic poison and enzyme, and it can damage the central nervous system and accumulate in the bones, brain, kidney, and muscles in humans (2). It is very important to remove these heavy metal pollutants from industrial wastewater.

Various methods have been used for removal and recovery of metal industry wastewater such as reverse osmosis, ion exchange, chemical precipitation, adsorption and membrane filtration (3). Among these methods, adsorption is the most preferred method for the removal of heavy metal pollutions from industrial wastewater. Adsorption has the advantages of low cost, high selectivity, environment-friendly, reusable adsorbent design, and easy usability.

Diatomite is a fine sedimentary rock of biogenetic origin with $SiO_2 \cdot nH_2O$ formula that is mainly composed of the siliceous skeletal remains of diatoms (4). Diatomite has unique physicochemical

properties, such as highly developed mesoporosity and/or macroporosity, hydrophobia, charge, solubility, ion exchange, acidity and high adsorptive capabilities (5). So, it is used as an effective adsorbent in the removal of heavy metal pollutants and toxic organic pollutants from industrial wastewater (6).

Chitosan is one of the most important natural polymers in nature. It is often used in the structure of many composite materials. Chitosan is used as an effective adsorbent in the removal of heavy metal ions due to their hydrophilicity, biodegradability, non-toxicity, and has hydroxyl and a large number of amino groups (7).

The literature review shows that many studies have been conducted about the removal of lead. A series of recent studies; Fan et al., (8) chitosan/graphene oxide composite, Senol et al., (9) chitosan/vermiculite composite, Sun et al., (10) chitosan/cellulose composite, Gupta et al., (11) chitosan/ hydroxyapatite composite, Titom et al., (12) chitosan/clay composite have examined for removal of lead ions by adsorption. However, there is no reported study on the use of chitosan-diatomite composite in the removal of lead ions.

Chitosan can be dissolved under acidic conditions, although it does not have a solubility in alkaline and neutral media. So, this condition limits the use of chitosan as an adsorbent. But it can be possible to use chitosan as an adsorbent with generated composites. A new approach is therefore needed for a useful, cost-effective, water-insoluble, non-toxic, and natural polymer/mineral adsorbent. Within this scope, Ch-D composite was synthesized using chitosan (Ch) biopolymer and diatomite (D) mineral. Thus, the practicality of use for chitosan was provided. The adsorbent properties of Ch-D composite for the removal of lead ion from aqueous medium were investigated. The characterizations of the newly synthesized adsorbent were performed by FTIR, SEM-EDX, and point of zero charge (PZC) analyses. Adsorption properties were investigated for lead ions from aqueous solution. The effect of solution pH, initial Pb^{2+} concentration, temperature, contact time and recovery on adsorption were considered and optimum conditions were determined.

MATERIALS AND METHODS

Chemicals and Devices

In this study, medium molecular weight chitosan (Ch) (Sigma-Aldrich, Germany) was preferred. The natural diatomite was supplied from Akmin Mining (Ankara). $Pb(NO_3)_2$, 4-(2-pyridylazo) resorcinol (PAR) and other chemicals were achieved from Merck (Germany). Double-distilled water used in all dilutions and experiments. The lead concentration was determined using a UV-vis spectrophotometer (SHIMADZU, 160 A model, Japan).

Characterization techniques

Ch, D, and Ch-D were characterized by FT-IR and SEM-EDX analysis. FT-IR spectra of Ch-D and its components were recorded in a Perkin Elmer 400 spectrometer. SEM images and EDX compositional data of Ch-D composite and its components were obtained with a Leo 440 Computer Controlled Digital System.

Synthesis of Ch-D Composite

To synthesize about 4 g of Ch-D composite, 2 g of chitosan and 2 g of diatomite were mixed in a 5% (v/v) acetic acid solution for 2 hours until a homogeneous mixture was obtained. Then a solution of epichlorohydrin (ECH) was added and stirred. The mixture was then added dropwise to the sodium tripolyphosphate (NaTPP) solution to form composite beads. The resulting beads were washed with double-distilled water until the conductivity of the wash water reached approximately the conductivity of double-distilled water. The samples dried in the oven at 40 °C were ground and stored in closed containers for later use.

UV-Vis spectrophotometric method

The concentration of Pb^{2+} ions was determined by measuring the UV-Vis spectrophotometric method of the complex formed by PAR (13). PAR was used as a complex-forming reagent for the determination of Pb^{2+} in the supernatants. A solution of 3.5×10^{-3} mol L^{-1} of PAR in 0.7 mol L^{-1} of Tris/HCl at pH 8–9 was prepared. A 50 μL fraction of supernatant was added onto 3 mL of the reagent and the absorbance of the formed metal complex was measured at λ = 518.5 nm for Pb^{2+}.

Batch adsorption procedure

The adsorption of Pb^{2+} ions onto Ch-D composite adsorbent was investigated in batch adsorption experiments. The stock solution of Pb^{2+} (1000 mg L^{-1}) was prepared using double-distilled water. The adsorbent-solution systems were equilibrated with 500 mg L^{-1} (2.4×10^{-3} mol L^{-1}) Pb^{2+} concentration at natural pH 4.0, for 24 h at 25 °C in 10 mL polypropylene tubes containing 10 mL of Pb^{2+} solution. Pb^{2+} ion concentration was determined by the absorbance measurement. The batch adsorption conditions are given in Table 1. Adsorption% and Q (mol kg^{-1}) were calculated with Eq. 1 and Eq. 2.

$$Adsorption\% = \left[\frac{C_i - C_f}{C_i}\right] x\, 100 \qquad \text{Eq. 1}$$

$$Q = \left[\frac{C_i - C_f}{m}\right] x\, V \qquad \text{Eq. 2}$$

Where, C_i is the initial concentration (mg L^{-1}), m refers to the adsorbent mass (g), C_f is equilibrium concentration (mg L^{-1}), and V is the solution volume (L).

Table 1. Batch adsorption experiment conditions for Pb^{2+} adsorption onto Ch-D

Experiment	Solution pH	Initial Pb^{2+} conc. (mg L^{-1})	Contact time (min)	Temperature (^{0}C)
Effect of pH	1.0-5.0	500	1440	25
Effect of concentration	4.0	50-800	1440	25
Effect of time	4.0	500	2-1440	25
Effect of temperature	4.0	500	1440	5, 25, 40
Desorption	4.0	500	1440	25

Desorption experiments

Desorption studies were performed for adsorbent recovery and re-use in adsorption processes. In this study, dilute 0.1 mol L^{-1} HCl, 0.1 mol L^{-1} NaOH, 0.1 mol L^{-1} HNO$_3$ and 0.1 mol L^{-1} ethyl alcohol solutions were used for desorption of the Pb^{2+} ions from the surface of the Ch-D. To determine the recovery property of the adsorbent, the experiments were repeated three times with the same adsorbent for the adsorbent/desorption cycle. At the end of each experiment, the solutions were centrifuged at 5000 rpm for 10 minutes to ensure liquid-solid separation and the amount of Pb^{2+} ions in the equilibrium solution was determined by UV-Vis spectrophotometric method. % Desorption was calculated with Eq. 3.

$$Desorption\% = \frac{Q_{des}}{Q_{ads}} x\, 100 \qquad \text{Eq. 3}$$

In the equation, Q_{des} is the desorbed amount of adsorbate (mol kg^{-1}), and Q_{ads} is the adsorbed amount of adsorbate (mol kg^{-1}).

Equilibrium isotherm studies
The adsorption isotherms are very useful to describe the interaction between the adsorbate and the adsorbent. The adsorption of Pb^{2+} ions onto Ch-D was modeled using the Langmuir, Freundlich, and Dubinin-Radushkevich (D-R) isotherm models (14, 15). The Langmuir, Freundlich, and Dubinin-Radushkevich (D-R) isotherm equations are expressed below (Eq. 4, Eq. 5 and Eq. 6, respectively).

$$Q = \frac{X_L K_L C_e}{1 + K_L C_e} \qquad \text{Eq. 4}$$

$$Q = K_F C_e^n \qquad \text{Eq. 5}$$

$$Q_e = Q_{DR} e^{-K_{DR}\varepsilon^2} \qquad \text{Eq. 6}$$

where Q (mol kg^{-1}) is the amount of adsorbed metal ions, X_L is the maximum adsorption capacity, K_L is the parameter for Langmuir isotherm and C_e is the equilibrium concentration (mol L^{-1}) and K_F: Freundlich constant, β: adsorbent surface heterogeneity. X_{DR} is a measure of adsorption capacity, K_{DR} is the activity coefficient (mol^2 K J^2) and ε is the Polanyi potential, R is the ideal gas constant (8.314 J mol^{-1} K^{-1}) and T is the absolute temperature (K). The Polanyi potential (ε) is expressed by Eq. 7:

$$\varepsilon = RT\ln\left(1 + \frac{1}{C_e}\right) \qquad \text{Eq.7}$$

The adsorption energy (E) is expressed by the following Eq. 8:

$$E_{DR} = \left(2 K_{DR}\right)^{-0.5} \qquad \text{Eq. 8}$$

If the adsorption energy is 8<E<16 kJ mol^{-1}, the adsorption is physically controlled and E<8 kJ mol^{-1} indicates that the adsorption proceeds physically (16, 17).

Kinetics studies
The three most commonly used kinetics models were used to evaluate the contact time dependence of the adsorption process (18, 19). The adsorption kinetics of Pb^{2+} ions onto Ch-D were described by pseudo-first-order (PFO),

pseudo-second-order (PSO) and intraparticle diffusion (IPD) kinetic models equations (Eq. 9, Eq. 10 and Eq. 11, respectively).

$$Q_t = Q_e[1 - e^{-k_1 t}] \qquad \text{Eq. 9}$$

$$Q_t = \frac{t}{\left[\dfrac{1}{k_2 Q_e^2}\right] + \left[\dfrac{t}{Q_e}\right]} \qquad \text{Eq. 10}$$

$$Q_t = k_i t^{0.5} \qquad \text{Eq. 11}$$

where Q_t (mol kg^{-1}) is the lead absorbed amount at time t (min), Q_e (mol kg^{-1}) is the absorbed amount at equilibrium, k_1, k_2 and k_i is the rate constant of the PFO (min^{-1}), the PSO model (mol^{-1} kg min^{-1}) and the intra-IPD (mol^{-1} kg min$^{-0.5}$) model, respectively.

Thermodynamic studies

Thermodynamic parameters are used to explain the effect of the temperature on the adsorption. Enthalpy and entropy (ΔH^0 and ΔS^0) are obtained from lnK_D against the 1/T graph. The slope (-ΔH^0/R) and y-intercept (ΔS^0/R) of the data plotted as lnK_D against the 1/T graph. The free Gibbs energy (ΔG^0) is calculated from Equation 15. ΔH^0, ΔS^0, and ΔG^0 were calculated using the following equations:

$$K_D = \frac{Q}{C_e} \qquad \text{Eq.12}$$

$$\Delta G = -RT \ln K_D \qquad \text{Eq.13}$$

$$\ln K_D = \frac{\Delta S^0}{R} - \frac{\Delta H^0}{RT} \qquad \text{Eq.14}$$

$$\Delta G^0 = \Delta H^0 - T \Delta S^0 \qquad \text{Eq.15}$$

RESULTS AND DISCUSSION

FT-IR analysis

The FT-IR spectra of the D, Ch and Ch-D composite are given in Figure 1. When the FT-IR spectrum of the diatomite was examined, it is observed that the absorption peak at 1103, 1015 cm^{-1} showed the –Si–O–Si– vibration, the peak at 913 cm^{-1} showed the Si–O stretching, the peak at 796 and 694 cm^{-1} showed the SiO–H vibration, and the peaks at 537 and 469 cm^{-1} showed the Si–O–Si bonding vibration [20-22]. Additionally, the wide peak between the wavelengths of 1640-3600 cm^{-1} is assigned to the H-O-H and OH groups. In the FT-IR spectra of chitosan, bands between 3290-3350 cm^{-1} are associated with the OH and NH groups and 2864 cm^{-1} is observed the characteristic Ch peak. Peaks corresponding to the 1650 and 1575 cm^{-1} wavenumbers correspond to amide C-O and amide N-H groups, 1070 cm^{-1} attributed to the C-O bond which are characteristic peaks for Ch [23]. When the FT-IR spectrum of Ch-D composite is examined, it is seen that it is different from both spectra. The spectrum of Ch-D composite is observed in the characteristic peaks of both Ch and D.
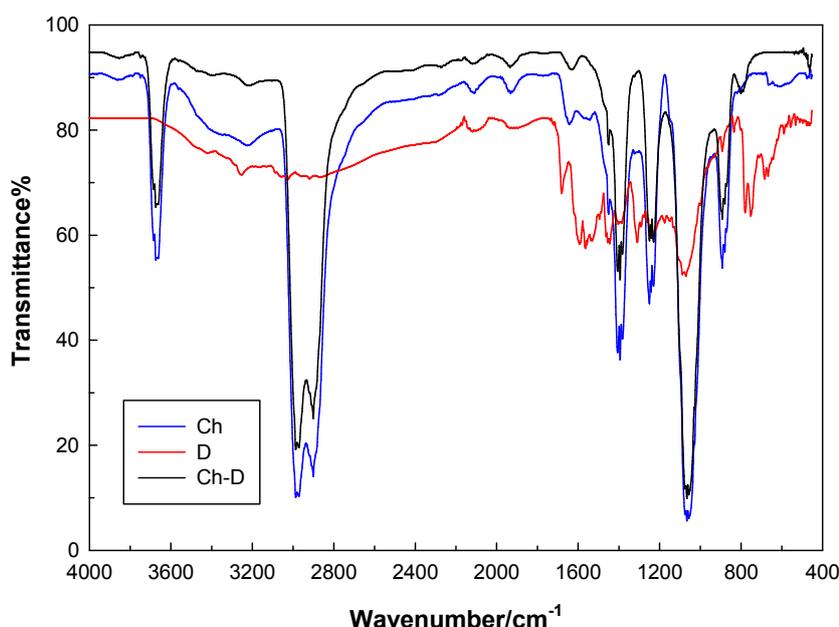

Figure 1. FT-IR spectra of Ch, D, and Ch-D.

When the FT-IR spectrum before and after Pb^{2+} adsorption was examined, peak intensities increased (Figure 2). Although the location of the peaks after Pb^{2+} adsorption did not change, peak intensity increased after Pb^{2+} adsorption. Changes in FT-IR spectra obtained before/after Pb^{2+} adsorption on Ch-D were considered as evidence for Pb^{2+} adsorption.
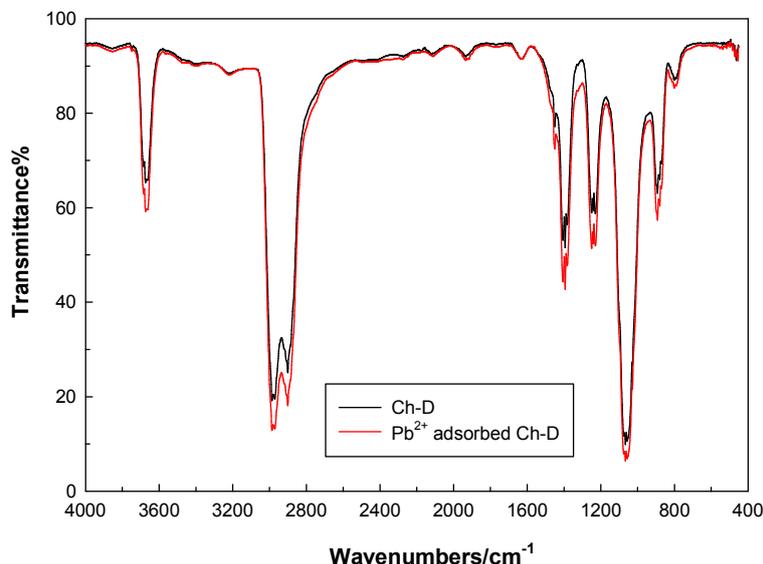
Figure 2. FT-IR spectra before and after adsorption.

SEM-EDX analysis

Microphotographs of Ch, D, and Ch-D are shown in Figure 3. The microphotograph of diatomite shows diatoms that generally have cylindrical, sheet-like shapes, and a porous structure (24). Microphotograph of Ch-D shows a structure having the structure of both Ch and D. EDX results of Ch, D, and Ch-D in Figure 3. EDX techniques show that the Ch mainly consists of C (52.8%), O (36.6%), N(10.6%) the D consists of O (53.7%) and Si (46.3%). The C, O, Si and N contents of Ch-D are the evidence of the presence of Ch and D.

Scanning electron microphotographs of Ch-D, before and after adsorption were shown in Figure 4. After adsorption, Pb^{2+} ions were coated on the surface of the chitosan–diatomite. Changes in SEM images obtained before/after Pb^{2+} adsorption on Ch-D were considered as evidence for Pb^{2+} adsorption. On the other hand, the Pb content in EDX spectra of Ch-D is evidence of adsorption of Pb^{2+} onto Ch-D.
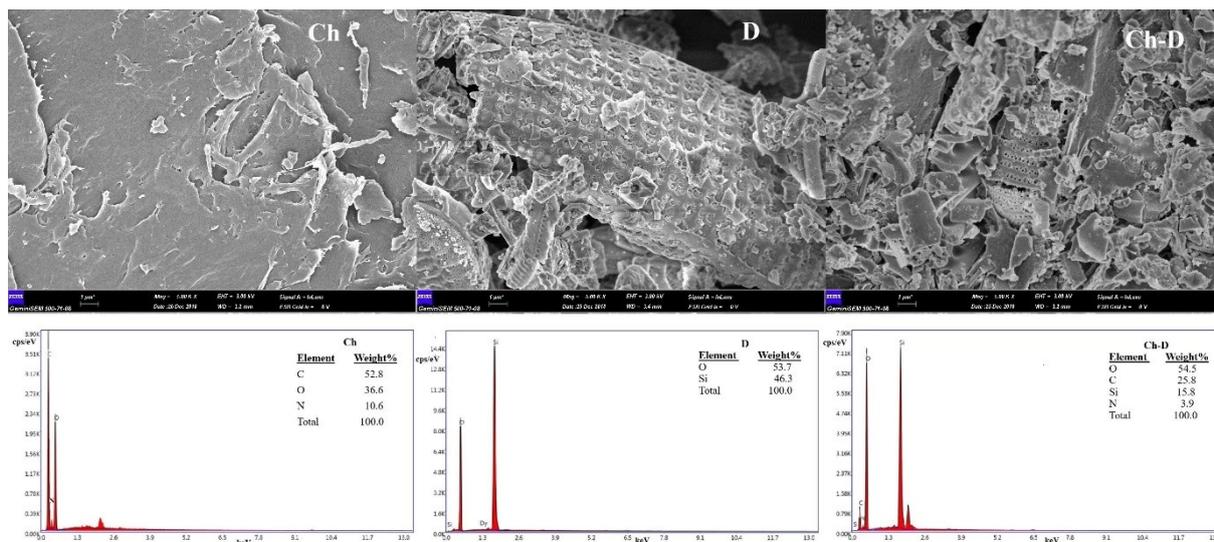
Figure 3. Scanning electron microphotographs of Ch, D, and Ch-D and EDX results of Ch, D, and Ch-D.
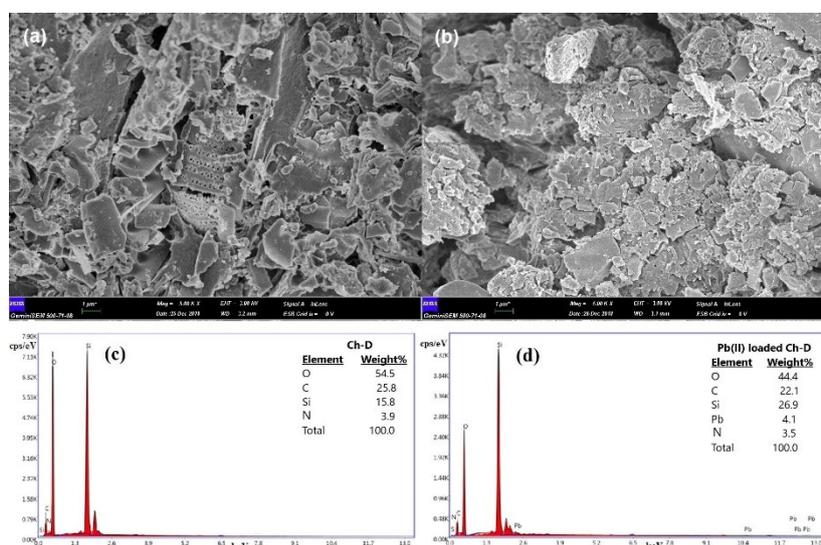

Figure 4. Scanning electron microphotographs of Ch-D (a) and Pb^{2+} adsorbed Ch-D (b) and EDX results of Ch-D (c) and Pb^{2+} loaded Ch-D (d).

Effect of pH

The adsorption mechanism is related to the physicochemical interactions of the species in solution. At high acidic pHs, metal cations and hydrogen ions compete for binding to active sites, resulting in less adsorption of the metal. At high basic pH values, soluble hydroxide complexes of metal ions are formed, so the adsorption is reduced.

To investigate the pH effect, adsorption studies were carried out at different pHs at constant Pb^{2+} ion concentration and results are presented in Figure 5. According to Figure 5, the percentage of the adsorption rate increased from 5% to 61% with increasing pH values from 1.0 to 4.0, respectively. The maximum adsorption rate was found as 61% at pH 4.0, which was the natural pH of the Pb^{2+} solution and was found to be the pH at which the adsorption was highest. Therefore, all adsorption experiments were performed at the natural pH of the Pb^{2+} ion. Pb^{2+} ions can precipitate at alkaline pHs as hydroxides. So, pHs beyond 5.0 were not studied.
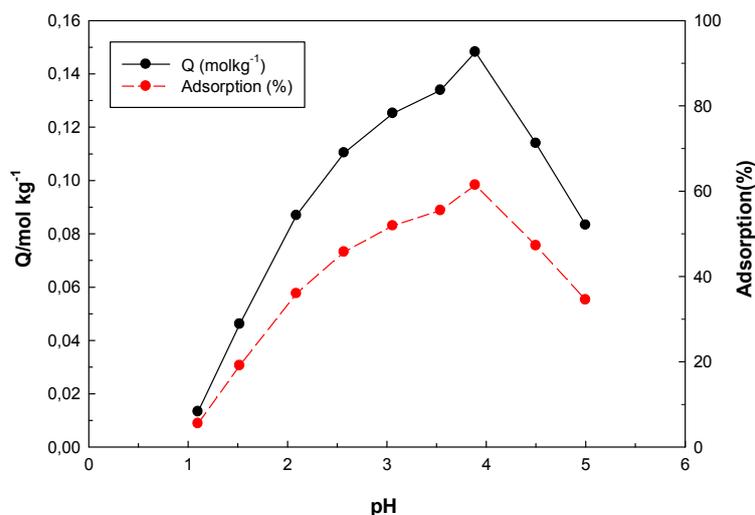
Figure 5. Effect of pH on adsorption of Pb^{2+} onto Ch-D (at 25°C; adsorbent dose:100 mg; C_0:500 mg L^{-1}).

To determine the point of zero charge (PZC) values of Ch-D composite, 100 mg Ch-D was held in solutions in the pH = 1.0-12.0 range by NaOH and HCl at 25 ^{0}C for 24 h and the equilibrium pH was measured. The results are given in Figure 6. The surface charge of the Ch-D composite adsorbent was found to be positively charged, under pH 4.63 and negatively charged above pH 4.63 (25).
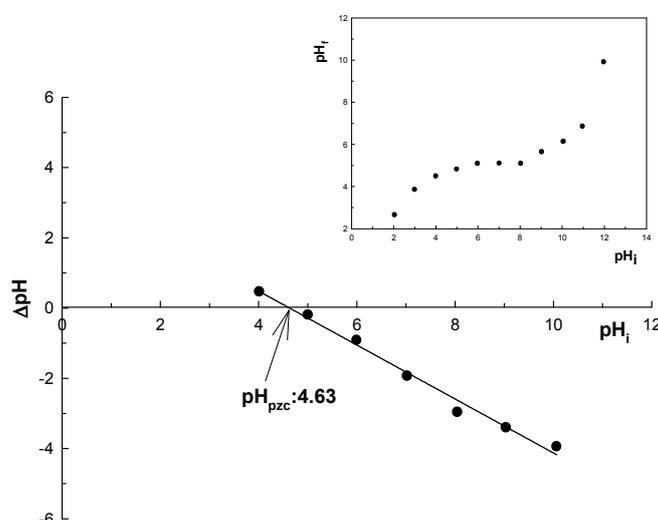

Figure 6. PZC plots of the Ch-D composite.

Adsorption isotherms

The harmony of the Langmuir, Freundlich, and Dubinin-Radushkevich isotherm models was presented in Figure 5 and Table 2, with the parameters used in the isotherms. The maximum adsorption capacity was calculated to be 0.154 mol kg^{-1} from the Langmuir isotherm model. Pb^{2+} adsorption onto Ch-D fitted well the Freundlich model. The Freundlich parameter n indicates the degree of heterogeneity of the surface and the E_{DR} value found in the D-R model indicates that the adsorption process is chemical.
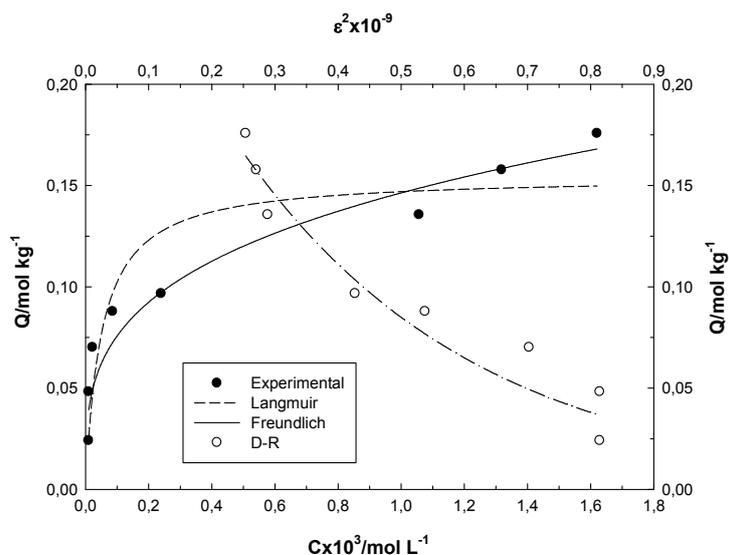
Figure 7. Langmuir, Freundlich, and D-R isotherm plot for the adsorption of Pb^{2+} onto Ch-D (at 25 °C; adsorbent dose:100 mg; C_0:50-800 mg L^{-1}).

Table 2. Adsorption isotherm parameters.

Langmuir		Freundlich		D-R	
X_L/mol kg^{-1}	0.154	K_f	1.06	X_{DR}	0.326
K_L/L mol^{-1}	19570	β	0.286	$-K_{DR}x10^6$	2.69
R^2	0.882	R^2	0.927	R^2	0.932
				E/kJ mol^{-1}	13.6

Standard Deviation 0.053 mol kg^{-1}, Standard Error 0.018 mol kg^{-1}

Adsorption kinetics

Adsorption data for kinetics studies were performed in the time range of 2-1440 min. The adsorption kinetics of Pb^{2+} onto Ch-D composite were presented in Figure 8 and Table 3. From the regression coefficient (R^2) and the harmony of theoretically calculated Q_t and experimental Q_e values, it was concluded that the PFO model was a suitable model for the adsorption kinetics of Pb^{2+} ions on the Ch-D composite adsorbent.
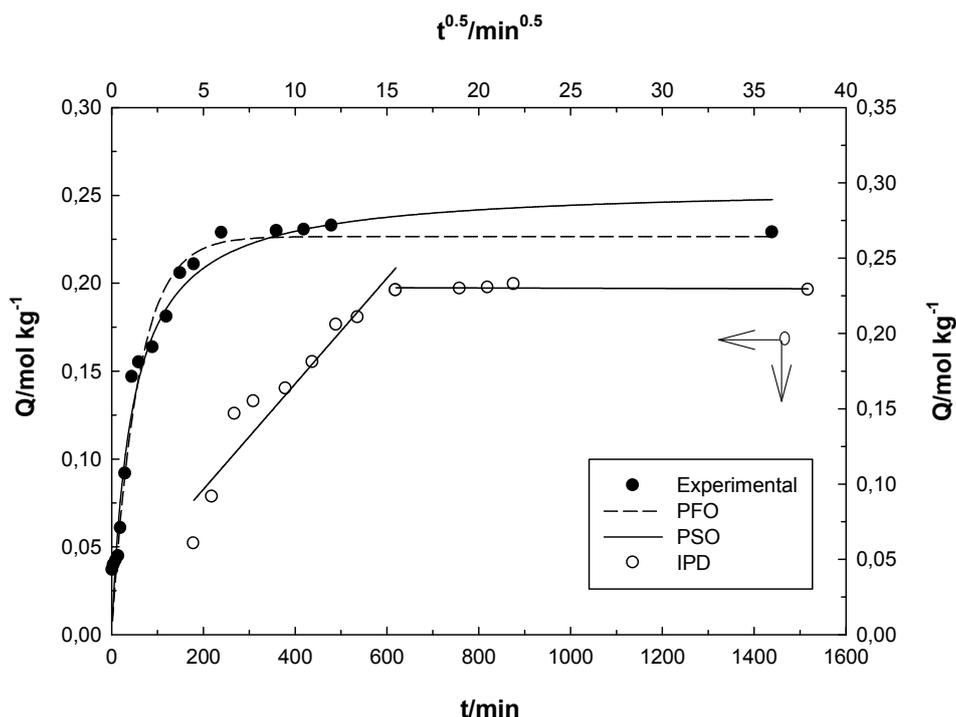
Figure 8. Compatibility of Pb^{2+} adsorption kinetics to PFO, PSO and IPD models (at 25°C; adsorbent dose:300 mg; C_0:500 mg L^{-1}).

Table 3. Adsorption kinetic parameters.

Pb^{2+}	$(k_1, k_2, k_i) \times 10^3$	R^2	Q_t	Q_e	$H \times 10^3$
PFO	57.5	0.972	0.228	0.227	3.97
PSO	58.1	0.971	0.228	0.313	5.69
IPD	25.7	0.905	-	-	-

Standard Deviation 0.078 mol kg^{-1}, Standard Error 0.019 mol kg^{-1}

Adsorption thermodynamics

To explain the thermodynamic behavior of Pb^{2+} ions adsorption onto the Ch-D composite, it was studied at temperatures of 5 ^{0}C, 25 ^{0}C, and 40 ^{0}C and Figure 9 was obtained. In Figure 9 (ln K_D-1/ T) the values of ΔH^0 and ΔS^0 were calculated from the slope of the graph and the cut-off, respectively.

Adsorption enthalpy was found negative. ΔH^0 was calculated as -11.3 kJ mol^{-1} showed that the adsorption process was exothermic. ΔS^0 was calculated as 2.29 J mol^{-1} K^{-1}. The free energy value was found as -12.0 kJ mol^{-1} at 25 ^{0}C. The negative free energy value indicated that spontaneous adsorption was possible.
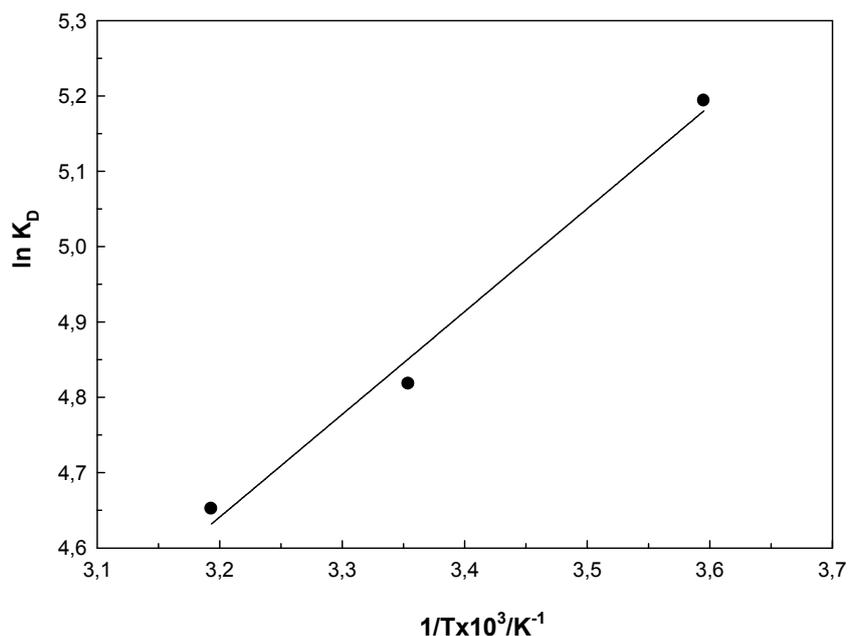
Figure 9. Effect of temperature on the adsorption. (at 5°C, 25°C, 40°C; adsorbent dose:100 mg; C_0:500 mg L^{-1})

Desorption

Reusability investigated the desorption ability for Pb^{2+} ions onto Ch-D composite. The Ch-D composite was regenerated using HCl, NaOH, HNO₃, and ethyl alcohol. The obtained Pb^{2+} removal efficiency for three times is plotted in Figure 10. The maximum recovery percentage for Pb^{2+} ions onto Ch-D was achieved with HCl (89%). The minimum recovery percentage for Pb^{2+} ions onto Ch-D was achieved with ethyl alcohol (11%).
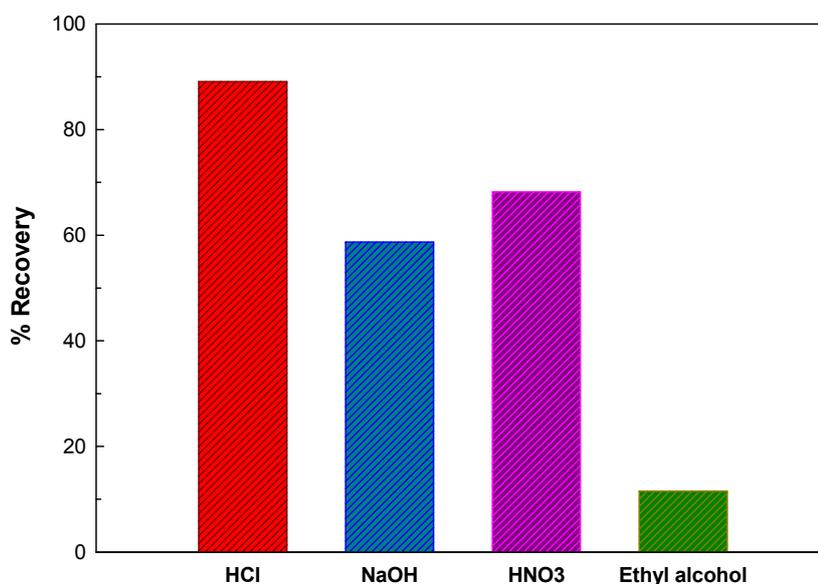

Figure 10. Recovery percents of HCl, NaOH, HNO₃ and ethyl alcohol for the desorption of Pb^{2+} onto Ch-D (at 25°C; adsorbent dose:100 mg; C_0:500 mg L^{-1}).

Comparison of results with literature

A comparison has been made between the chitosan composites adsorbents reported in the literature for the adsorption Pb^{2+}. The maximum adsorption capacity obtained from the Langmuir model was used for the comparison of different chitosan composite adsorbents. As can be seen in Table 4, the maximum adsorption capacity of chitosan-diatomite composite adsorbent (0.154 mol kg^{-1}) was higher than that of various chitosan composite adsorbents.

Table 4. Comparison of Pb^{2+} adsorption on the chitosan-diatomite composite with other chitosan composite adsorbents.

Adsorbent	$X_L/molkg^{-1}$	Reference
Chitosan-graphene oxide	0.372	(8)
Chitosan-vermiculite	0.598	(9)
Chitosan-cellulose	0.130	(10)
Chitosan-hydroxyapatite	0.058	(11)
Chitosan–clay	0.156	(12)
Chitosan-sand	0.060	(26)
Chitosan-bentonite	0.382	(27)
Chitosan-diatomite	0.154	(This study)

CONCLUSIONS

In this investigation, Ch-D composite can be used as an effective, alternative adsorbent for the removal of Pb^{2+} ions. Optimal conditions of the study for the adsorption were determined and were selected as pH:4.0, m:100 mg, t:24 h, and T:25 ^{0}C. The Freundlich model was found to be the better fit to the experimental data. The maximum adsorption capacity was found to be 0.154 mol kg^{-1} from the Langmuir isotherm model. Adsorption thermodynamics indicated that the adsorption process was exothermic, possible and spontaneous. Ch-D composite adsorbent had a well adsorption-desorption ability for Pb^{2+} ions. Ch-D composite can use as an effective and alternative adsorbent in the removal of lead pollutants from industrial wastewater.

ACKNOWLEDGMENT

REFERENCES

1. Paulino AT, Minasse FAS, Guilherme MR, Reis AV, Muniz EC, Nozaki J. Novel adsorbent based on silk worm chrysalides for removal of heavy metals from wastewaters. Journal of colloid and interface science 2006;301(2):479-87.

2. Fu F, Wang Q. Removal of heavy metal ions from wastewaters: A review. Journal of environmental management. 2011;92(3):407-18.

3. Benito Y, Ruiz ML. Reverse osmosis applied to metal finishing wastewater. Desalination. 2002; 142(3):229-34.

4. Al-Degs Y, Khraisheh MAM, Tutunji MF. Sorption of lead ions on diatomite and manganese oxides modified diatomite. Water Research. 2001;35(15):3724-8.

5. Deng L, Du P, Yu W, Yuan P, Annabi-Bergaya F, Liu D, Zhou J. Novel hierarchically porous allophane/diatomite nanocomposite for benzene adsorption. Applied Clay Science. 2019;*168*:155-63.

6. Senol ZM, Arslan DS, Simşek S. Preparation and characterization of a novel diatomite-based composite and investigation of its adsorption properties for uranyl ions. Journal of Radioanalytical and Nuclear Chemistry. 2019;321(3):791-803.

7. Vakili M, Deng S, Liu D, Li T, Yu, G. Preparation of aminated cross-linked chitosan beads for efficient adsorption of hexavalent chromium. International journal of biological macromolecules. 2019;139:352-60.

8. Fan L, Luo C, Sun M, Li X, Qiu H. Highly selective adsorption of lead ions by water-dispersible magnetic chitosan/graphene oxide composites, Colloids and Surfaces B: Biointerfaces. 2013;103:523-9.

9. Senol ZM. Kitosan-Vermikülit Kompoziti Kullanılarak Sulu Çözeltiden Etkin Kurşun Giderimi: Denge, Kinetik ve Termodinamik Çalışmalar, Academic Platform Journal of Engineering and Science. 2020;8(1):15-21.

10. Sun X, Peng B, Ji Y, Chen J, Li D. Chitosan(chitin)/cellulose composite biosorbents prepared using ionic liquid for heavy metal ions adsorption. AIChE Journal. 2009;55(8):2062–2069.

11. Gupta N, Kushwaha AK, Chattopadhyaya MC. Adsorptive removal of Pb^{2+}, Co^{2+} and Ni^{2+} by hydroxyapatite/chitosan composite from aqueous solution. Journal of the Taiwan Institute of Chemical Engineers, 2012;43(1):125-31.

12. Tirtom VN, Dinçer A, Becerik S, Aydemir T, Çeli A. Comparative adsorption of Ni(II) and Cd(II) ions on epichlorohydrin crosslinked chitosan–clay composite beads in aqueous solution. Chemical Engineering Journal, 2012;197:379-86.

13. Senol ZM, Gül ÜD, Şimşek S. Assessment of Pb^{2+} removal capacity of lichen (Evernia prunastri): application of adsorption kinetic, isotherm models. and thermodynamics. Environmental Science and Pollution Research. 2019;26(26):27002-13.

14. Langmuir J. The adsorption of gases on plane surfaces of glass, mica and platinum I. Journal of the American Chemical Society. 1918;40:1361-1403.

15. Helfferich F. Ion exchange. McGraw Hill. New York. 1962;166.

16. Dubinin MM. The potential theory of adsorption of gases and vapors for adsorbents with energetically non-uniform surface. Chemical Reviews. 1960; 60:235–66.

17. Hobson JP. Physical adsorption isotherms extending from ultra-high vacuum to vapor pressure. The Journal of physical chemistry. 1969;73:2720–7.

18. Cui X, Hao H, Zhang C, He Z, Yang X. Science of the total environment capacity and mechanisms of ammonium and cadmium sorption on different wetland-plant derived biochars. Science of the Total Environment. 2016;539:566–75.

19. Inyang M, Gao B, Ding W, Pullammanappallil P, Zimmerman AR, Cao X. Enhanced Lead sorption by biochar derived from anaerobically digested sugarcane bagasse. Separation Science and Technology. 2011;46:1950–6.

20. Sharma P, Tomar R. Synthesis and application of an analogue of mesolite for the removal of uranium (VI), thorium (IV), and europium (III) from aqueous waste. Microporous and Mesoporous Materials, 2008;*116* (1-3):641-52.

21. Sheng G, Hu J, Wang X. Sorption properties of Th (IV) on the raw diatomite—effects of contact time, pH, ionic strength and temperature. Applied Radiation and Isotopes, 2008; 66(10):1313-20.

22. Khraisheh MA, Al-degs YS, Mcminn WA. Remediation of wastewater containing heavy metals using raw and modified diatomite. Chemical Engineering Journal. 2004;99(2):177-84.

23. Pawlak A, Mucha M. Thermogravimetric and FTIR studies of chitosan blends. Thermochimica Acta. 2003;396(1-2):153-66.

24. Sprynskyy M, Kovalchuk I, Buszewski B. The separation of uranium ions by natural and modified diatomite from aqueous solution. Journal of Hazardous Materials. 2010; 181(1-3):700-7.

25. Čerović LS, Milonjić SK, Todorovi, MB, Trtanj MI, Pogozhev YS, Blagoveschenskii Y, Levashov EA. Point of zero charge of different carbides. Colloids and Surfaces A: Physicochemical and Engineering Aspects. 2007;297(1-3):1-6.

26. Ngah WW, Teong L, Hanafiah M. Adsorption of dyes and heavy metal ions by chitosan composites: A review. Carbohydrate Polymers, 2011;83(4):1446–56.

27. Ska DK. Chitosan as an effective low-cost sorbent of heavy metal complexes with the polyaspartic acid. Chemical Engineering Journal, 2011;173:520-9.